Thermodynamic and Performance Assessment of an Innovative Solar-Assisted Tri-Generation System for Water Desalination, Air-Conditioning, and Power Generation

A. Fouda
Department of Mechanical and Materials Engineering
Faculty of Engineering, University of Jeddah
Jeddah, Saudi Arabia
aafoudah@uj.edu.sa

H. F. Elattar
Department of Mechanical and Materials Engineering
Faculty of Engineering, University of Jeddah
Jeddah, Saudi Arabia
hfalattar@uj.edu.sa

Saeed Rubaiee
Department of Mechanical and Materials Engineering
Department of Industrial and Systems Engineering
Faculty of Engineering, University of Jeddah
Jeddah, Saudi Arabia
salrubaiee@uj.edu.sa

Abdullah S. Bin Mahfouz
Department of Chemical Engineering
Faculty of Engineering, University of Jeddah
Jeddah, Saudi Arabia
asbinmahfooz@uj.edu.sa

Abdullah M. Alharbi
Department of Industrial and Systems Engineering
Faculty of Engineering, University of Jeddah
Jeddah, Saudi Arabia
amealharbi@uj.edu.sa

Received: 3 August 2022 | Revised: 14 August 2022 | Accepted: 15 August 2022

Abstract-An innovative tri-generation system powered by solar energy for water desalination, air-conditioning, and electrical power production is proposed and investigated numerically in this paper. The system is designed for small and medium-sized buildings in countries that are rich in solar energy but poor in fossil fuels and water resources. The devised system includes a solar system (evacuated tube collectors and thermal energy storage unit), an Organic Rankine Cycle (ORC), a Humidification and Dehumidification (HDH) water desalination system, and a Desiccant Cooling System (DCS). A detailed parametric study of the developed system is carried out for a wide range of operating conditions and design parameters on the system's productivity and performance parameters. It is found that: (i) The proposed tri-generation system can deliver high electrical power, fresh water, space cooling capacity, and Energy Utilization Factor (EUF) of 104.5kW, 72.37kg/h, 25.48kW, and 0.2643 respectively. In comparison to the basic system, the EUFimp and ASC,sav parameters were enhanced having maximum values of 69.9% and 41.14% respectively. General numerical correlations derived from the numerical data can predict the system productivity and performance parameters within reasonable error.

Keywords-tri-generation; organic Rankine cycle; humidification-dehumidification; desiccant cooling system

I. INTRODUCTION

Due to the increasing population and pollution, the needs for fresh water productivity, electricity generation, and air conditioning have dramatically increased. The heat rejection to the environment can be overcome by double-use systems that integrate desalination and power systems, in which the low-grade heat rejected from the power cycle is used to drive the desalination system. This significantly improves the energy efficiency of the combined plant [1-7]. On the other hand, dual solar-powered systems can play a key part in reducing CO_2 emissions. In addition, the integration of Concentrated Solar Power (CSP) and cogeneration systems can reduce the unit product costs of water and electricity with current developments in CSP technology [8]. Solar electricity and desalination systems can offer economic solutions to meet the increasing demands for both electricity and freshwater in dry arid regions such as the Gulf and MENA (Middle East and North Africa). To face the problem of rising temperatures, it is also necessary to adapt the air to achieve thermal comfort,

Corresponding author: A. Fouda

which can be accomplished by using a desiccant air conditioner, which is distinguished by not producing polluting gases such as chlorofluorocarbons, which are produced by traditional air conditioning systems. A hybrid system of air conditioning and desalination units was employed to lower the use of electricity in desalination and air conditioning systems. In hybrid air conditioners, renewable energy is also used to minimize the rate of power consumption. Several researchers combined air conditioning and refrigeration systems with HDH water desalination systems in different configurations to obtain hybrid systems for cooling and air conditioning [9–12]. The effects of system configuration, operating conditions, and geometric parameters have been investigated. Authors in [13] proposed a low-energy HDH and A/C hybrid system using an efficient design of dehumidifier (strips-finned helical coil) and packing pad material (cellulose paper in bee-hive structure). The integrated cooling or heating, fresh water generation and power systems, known as tri-generation plants, are an efficient method intended to have a lower consumption of primary energy and reduce greenhouse gas emissions. The processes and technologies for trigeneration that are currently available can provide a number of benefits [14, 15]: increasing global energy efficiency while expanding the use of renewable energy sources, lowering environmental impact in terms of carbon dioxide equivalent emissions, and reducing electrical system overloads and blackouts. Tri-generation techniques are used in several areas, including buildings, industries, and manufacturing [16].

Few researchers have concentrated on tri-generation system modeling. Previous research has looked into multi-generation facilities for electricity, cooling or heating, and freshwater generation that are combined with renewable energy resources. Authors in [17] investigated a multi-generation system that generates electrical power, freshwater, space cooling, and industrial heating using geothermal, solar, and ocean thermal energy conversion as energy inputs. Authors in [18] created a tri-generation facility that includes a flat plate solar collector field, a Kalina electrical power generation cycle, and a multi-stage desalination unit. A thermodynamic analysis of a polygeneration system comprising a Solar Power System (SPS), a Multi Effect Desalination (MED) system, and an Absorption Refrigeration System (ARS) was given in [19]. Solar energy is used to power the plant, which is supplemented by a natural gas heater. The impacts of various design and operating parameters on the plant's energy and exergetic parameters are investigated using a parametric study. Authors in [20] created a new tri-generation system for freshwater, electricity, and cooling production. A HDH unit is used as a binary cycle in this trigeneration system. According to the literature review, there are several cogeneration systems integrated with ORC/HDH and DCS/HDH, and a few trigeneration systems for power, freshwater, and cooling load integrated with MED/SRC/ARS and HDH/ORC/ECC, including CPVT, biogas, biomass boilers, and geothermal wells. So, tri-generation systems have not been extensively investigated up to now. For this aim, a new trigeneration set-up on the basis of an ORC, a DCS, and a HDH unit is designed to generate power, cooling, and freshwater. ORC power generation is only appropriate for small-scale applications and low operating temperatures [21]. Low-temperature energy utilization (e.g. waste energy, solar energy), simplicity, and low operating and installation costs are advantages of HDH water desalination. A desiccant air conditioner is a type of air conditioner that does not emit polluting gases like chlorofluorocarbons. CPVT, on the other hand, is an appealing technology due to its efficiency, but its dependability and economic feasibility have yet to be proven [22]. These restrictions inspire the authors to investigate the design of a tri-generation system that can supply small-scale continuous daylight electrical power, cooling, and desalination using solar energy sources.

The energy analysis of a tri-generation system comprising evacuated tube collectors, a thermal energy storage unit, an ORC, a HDH, and a DCS is presented in the current study. To the best of our knowledge, no previous research has looked into such a complex system. The paper will present the following that will help in the design of the proposed system: (i) Extensive energy mathematical modeling, (ii) the effect of various design and operating parameters on the proposed system's performance, (iii) evaluation of the system and comparison with the basic system, (iv) numerical correlations for the system's productivity and performance parameters in terms of the studied parameters.

II. SYSTEM DESCRIPTION

The proposed tri-generation system, depicted in Figure 1, can produce electricity, cooling, and potable water by combining ORC with DCS and an HDH desalination unit. The solar system includes an evacuated tube solar collector and a thermal storage tank. For the solar field loop, a thermal oil (Therminol-VP1) is used as a working fluid because it is able to remain in the liquid phase in temperatures up to 400°C [23]. The system can be decomposed into four main loops: two closed loops (solar fluid loop and ORC fluid loop) and two open loops (air loop and water loop). In the solar field loop, evacuated tubes solar collectors are used to gather the solar radiation through which the thermal oil flows, which is used to charge the storage tank during the sunlight period (state points 23 and 24). The thermal storage tank is used to supply the proposed system with constant demand during daylight. The thermal oil is used to transfer heat from/to the thermal storage tank to/from the ORC (i.e. evaporator) at state points 25 and 26. In the closed ORC fluid loop, heat is transferred from the secondary fluid to the ORC working fluid through the evaporator where it is boiled and superheated at state point 19. Then, the superheated ORC fluid expands in the turbine, producing the required electrical load in a generator. Low-grade superheated organic fluid (state point 20) is rejected from the turbine and sent to the condenser (triple channel heat exchanger) where it gets condensed at state point 17 and supplies the DCS and HDH units with the required heat to keep the temperature of state points 8 and 15 the same. After that, the ORC liquid is pressurized by the pump and sent to the evaporator (state point 18) for a gain and the cycle is completed. For the ORC in the present study, n-Octane was selected as the working fluid since it has the best performance among other organic fluids [24] due to its thermodynamic properties (e.g. Tcr = 296.2°C and Pcr = 2497kPa).

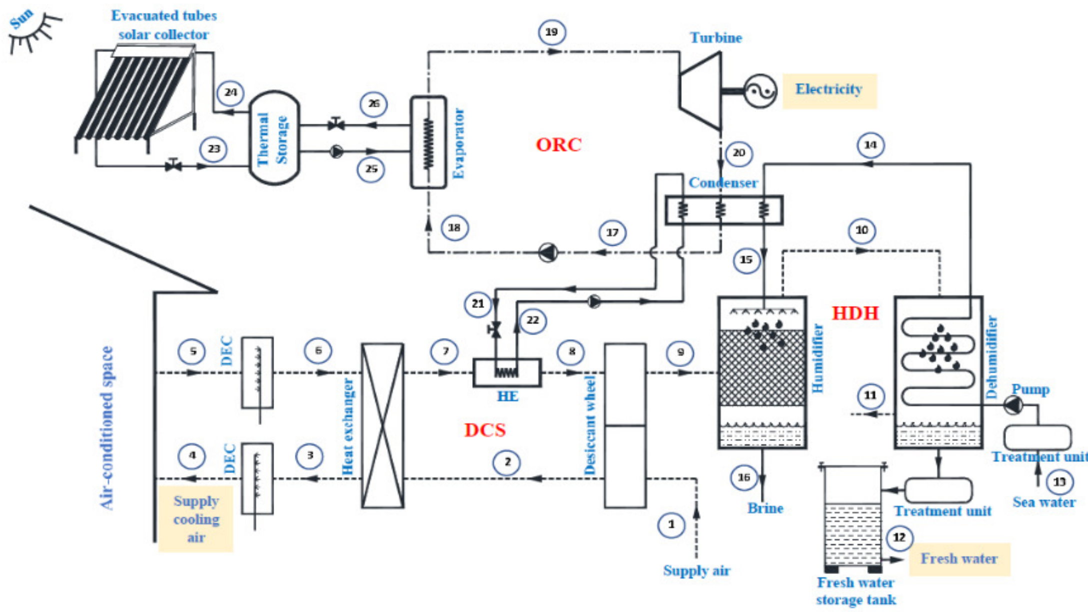

Fig. 1. Proposed tri-generation system layout.

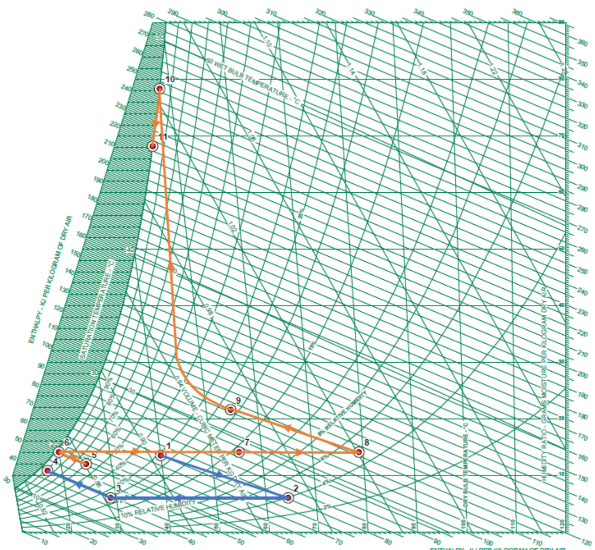

Fig. 2. Proposed tri-generation system psychrometric cycles.

In the air loop, process air enters the desiccant wheel at state point 1, where it is dehumidified and heated to state point 2. The process air input to the heat exchanger is at state point 2, and it is sensibly cooled to state point 3. After that, the process air enters the direct evaporative cooler at state point 3, where it is cooled and humidified before being delivered to the air-conditioned space at state point 4. At state point 5, the return air from the room inlet is directed to the direct evaporative cooler, where the air is cooled and humidified to state point 6. At this point, the return air inlet to the heat exchanger cools the process supply air, where the return air is sensible heated to state point 7. At state point 7, the return air (regeneration air) goes through the heat exchanger, which recovers a portion of the ORC condenser heat, and the regeneration air is sensibly heated to the desired regeneration temperature at state point 8. After that, the regeneration air from state point 8 enters the reactivation portion of the desiccant wheel, where it is cooled and humidified to state point 9 via the desiccant wheel. The humidifier receives the hot regeneration air from the desiccant wheel on a continual basis, humidifying it at state point 10 before flowing to the dehumidifier, where it is cooled and dehumidified at state point 11. In Figure 2, the psychrometric cycle depicts the passage of air through the proposed tri-generation system.

In the water loop, sea water at state point 13 is pumped by a feed water pump to the dehumidifier coil in order to dehumidify the process air for producing fresh water. The seawater exits the dehumidifier at state point 14, where it is preheated during the air dehumidification process. This preheated water flows through an ORC condenser and the heat recovered from the condenser is used to reheat the sea water to state point 15, and then it passes through the humidifier to humidify the air, where part of the water evaporates and is carried out of the humidifier by the incoming air, and the remaining part is drained as a brine at state point 16.

III. MATHEMATICAL MODEL AND THERMODYNAMICS ANALYSIS

The proposed tri-generation system is powered by solar energy for water desalination, air-conditioning, and power generation and it is integrated with a thermal energy storage unit. The system is simulated using the developed computer programs in C++ programming language and Engineering Equation Solver (EES) software based on the energy and mass balances for all system components. The tri-generation system is divided into three subsystems: ORC, HDH, and DCS in order to calculate the thermodynamic properties and subsystems and the whole system performance. In the simulating model procedure, the energy and mass conservation and first and second laws of thermodynamics are applied on each system components. The developed model is based on the following assumptions:

- All system processes are considered in steady state conditions.
- Leakage (air/water) in the system components is neglected.
- The temperatures of the blowdown water leaving the humidifier and the air wet-bulb temperature are equal.
- The mass flow rats of process air ($m^{\bullet}_{P,a}$), return air ($m^{\bullet}_{R,a}$), and water ($m^{\bullet}_{w}$) are equal.
- The temperatures of the air (t_8) and water (t_{15}) leaving the condenser of ORC are equal.
- The temperatures of the fresh water and the air wet-bulb at the dehumidifier exit are equal.
- The ORC fluid's state at the turbine inlet is superheated based on the different values of P_{18} and t_{19}
- The electrical generator efficiency of the ORC is 95%.
- The isentropic efficiency of the turbine and the pump is 75%.
- The effectiveness of all the heat exchangers is 80%.
- The efficiency of direct evaporative coolers used in the DCS is 90%.

In order to investigate and present the system performance, the Energy Utilization Factor (EUF), electrical power generation ($W^{\bullet}_{net}$), thermal efficiency of the ORC (η_{ORC}), fresh water productivity ($m^{\bullet}_{fresh}$), Gain Output Ratio (GOR), space cooling capacity ($Q^{\bullet}_{cooling}$), the coefficient of performance of DCS (COP_{DCS}), space supply air temperature and humidity ratio (t_4 and w_4), and area of solar collectors (A_{PSC}) are considered. In the present tri-generation system, electrical power, space cooling capacity, and fresh water productivity are being produced simultaneously from the single solar energy source.

A. Solar Radiation

The technique and complete calculation for obtaining the daily average solar intensity I_T for Jeddah are given in [25]. The I_T incidents on the surfaces of the air and water solar collectors (south oriented with a zero-tilt angle) are calculated for the weather conditions of Jeddah city, KSA on July 21 by regression analysis and are given by:

$$I_T\left(W/m^2\right)=10602.89\text{-}4332.31\tau+614.44\tau^2\text{-}34.45\tau^3\text{+}0.66\tau^4 \quad (1)$$

where τ represents the hour of day measured from 7:00 to 13:00. In the current work the daily average solar intensity is taken as $I_{T,avg,daily} = 750\,\text{W/m}^2$.

B. Organic Rankine Cycle

- Evaporator energy balance:

$$Q^{\bullet}_{Evap} = m^{\bullet}_{ORC}(h_{19} - h_{18}) \quad (2)$$

$$m^{\bullet}_{ORC}(h_{19} - h_{18}) = m^{\bullet}_{oil}(h_{25} - h_{26}) \quad (3)$$

$$\eta_{SC,PS} = \frac{Q^{\bullet}_{Evap}}{I_{T,avg,daily} A_{PSC}} \quad (4)$$

where the average annual value of thermal efficiency of the evacuated tube solar collector is 63.2% [75].

- Condenser energy balance:

$$Q^{\bullet}_{Cond} = m^{\bullet}_{ORC}(h_{20} - h_{17}) \quad (5)$$

$$\varepsilon_{HE} = \left(\frac{m^{\bullet}_{W}(h_{15} - h_{14}) + m^{\bullet}_{R,a}(h_8 - h_7)}{m^{\bullet}_{ORC}(h_{20} - h_{17})}\right) \quad (6)$$

$$MR = \frac{m^{\bullet}_{ORC}}{m^{\bullet}_{R,a} + m^{\bullet}_{w}} \quad (7)$$

- Turbine power:

$$W^{\bullet}_{t} = m^{\bullet}_{ORC}(h_{19} - h_{20})\eta_t\eta_g \quad (8)$$

- Pump power:

$$W^{\bullet}_{p} = m^{\bullet}_{ORC} v_{17}(P_{18} - P_{17}) / \eta_p \quad (9)$$

$$W^{\bullet}_{p} = m^{\bullet}_{ORC}(h_{18,a} - h_{17}) \quad (10)$$

- ORC net power and thermal efficiency:

$$W^{\bullet}_{net} = W^{\bullet}_{t} - W^{\bullet}_{p} \quad (11)$$

$$\eta_{ORC} = \frac{W^{\bullet}_{net}}{Q^{\bullet}_{Evap}} \quad (12)$$

C. Desiccant Cooling System

The desiccant wheel is the main component of the DCS. The model developed in [27] is carried out in the present work to simulate the desiccant wheel. The related energy balance and governing equations for the components of DCS are given below.

- Combined potential of the desiccant wheel:

$$F_{1,i} = \left[-\frac{2865}{\left(t_i + 273.15\right)^{1.49}}\right] + 4.344\left[w_i / 1000\right]^{0.8624} \quad (13)$$

$$F_{2,i} = \left[\frac{\left(t_i + 273.15\right)^{1.49}}{6360}\right] - 1.127\left[w_i / 1000\right]^{0.07969} \quad (14)$$

- Desiccant wheel's efficiency:

$$\eta_{F1} = \frac{F_{1,2} - F_{1,1}}{F_{1,8} - F_{1,1}} \quad (15)$$

$$\eta_{F2} = \frac{F_{2,2} - F_{2,1}}{F_{2,8} - F_{2,1}} \quad (16)$$

The efficiencies of the desiccant wheel are considered to be at the high level and about η_{F1} = 0.05 and η_{F2} = 0.95 [28].

- Energy and mass balances of the desiccant wheel:

$$\dot{m}_{P,a}(h_2 - h_1) = \dot{m}_{R,a}(h_8 - h_9) \quad (17)$$

$$\dot{m}_{P,a}(w_1 - w_2) = \dot{m}_{R,a}(w_9 - w_8) \quad (18)$$

- Heat exchanger:

$$\dot{m}_{P,a} c_{p,ma}(t_2 - t_3) = \dot{m}_{R,a} c_{p,ma}(t_7 - t_6) \quad (19)$$

$$\varepsilon_{HE} = \frac{\dot{m}_{P,a} c_{p,ma}(t_2 - t_3)}{C_{\min}(t_2 - t_6)} \quad (20)$$

where $C_{\min} = \min\{\dot{m}_{P,a} c_{p,ma}, \dot{m}_{R,a} c_{p,ma}\}$.

- Direct evaporative coolers:

$$\eta_{DEC(P,a)} = \frac{t_3 - t_4}{t_3 - t_{3,wb}} \quad (21)$$

$$\eta_{DEC(P,a)} = \frac{w_4 - w_3}{w_{4,Ideal} - w_3} \quad (22)$$

$$\eta_{DEC(R,a)} = \frac{t_5 - t_6}{t_5 - t_{5,wb}} \quad (23)$$

$$\eta_{DEC(R,a)} = \frac{w_6 - w_5}{w_{6,Ideal} - w_5} \quad (24)$$

- Regeneration energy, space cooling capacity, and coefficient of performance:

$$\dot{Q}_{in,DCS} = \dot{m}_{R,a}(h_8 - h_7) \quad (25)$$

$$\dot{Q}_{cooling} = \dot{m}_{P,a}(h_5 - h_4) \quad (26)$$

$$COP_{DCS} = \frac{\dot{Q}_{cooling}}{\dot{Q}_{in,DCS}} \quad (27)$$

D. Humidification Dehumidification System (HDH)

The energy balance of the humidifier is given as:

$$\dot{m}_{R,a}(h_{10} - h_9) = \dot{m}_w h_{15} - \dot{m}_{brine} h_{16} \quad (28)$$

where $\dot{m}_{brine} = \dot{m}_w - \dot{m}_{makeup}$.

The mass flow rate of the makeup water (sea or brackish water) supplied to the system is given as:

$$\dot{m}_{makeup} = \dot{m}_{R,a}(w_{10} - w_9) \quad (29)$$

The energy balance of the dehumidifier is given as:

$$\dot{m}_{R,a}(h_{10} - h_{11}) = \dot{m}_w(h_{14} - h_{13}) + \dot{m}_{fresh} h_{12} \quad (30)$$

$$\varepsilon_{deh} = \frac{\dot{m}_w c_{p,w}(t_{14} - t_{13})}{C_{\min}(t_{10} - t_{13})} \quad (31)$$

where $h_{12} = c_{p,w} t_{11}$ and $C_{\min} = \min\{\dot{m}_w c_{p,w}, \dot{m}_{R,a} c_{p,ma}\}$.

The condensate water mass flow rate leaving the dehumidifier is calculated as:

$$\dot{m}_{fresh} = \dot{m}_{R,a}(w_{10} - w_{11}) \quad (32)$$

The gain output ratio for the system is given by:

$$GOR = \frac{\dot{m}_{fresh}\ h_{fg}}{\dot{m}_w(h_{15} - h_{14}) + \dot{m}_{R,a}(h_9 - h_1)} \quad (33)$$

E. System Performance Parameters and Evaluation

The EUF of the proposed tri-generation and its corresponding basic system are expressed below:

$$EUF_{PS} = \frac{\dot{m}_{fresh}\ h_{fg} + \dot{Q}_{cooling} + \dot{W}_{net}}{\dot{Q}_{Evap}} \quad (34)$$

$$EUF_{BS} = \frac{\dot{m}_{fresh}\ h_{fg} + \dot{Q}_{cooling} + \dot{W}_{net}}{\dot{Q}_{Evap} + \dot{m}_W(h_{15} - h_{14}) + \dot{m}_{R,a}(h_8 - h_7)} \quad (35)$$

$$\eta_{SC,BS} = \frac{\dot{Q}_{Evap} + + \dot{m}_W(h_{15} - h_{14}) + \dot{m}_{R,a}(h_8 - h_7)}{I_{T,avg,daily} A_{bSC}} \quad (36)$$

For evaluating the system performance, the EUF improvement and the saving in the area of the solar collectors can be expressed as:

$$EUF_{imp} = \frac{EUF_{PS} - EUF_{BS}}{EUF_{BS}} \quad (37)$$

$$A_{SC,sav} = \frac{A_{SC,BS} - A_{SC,PS}}{A_{SC,BS}} \quad (38)$$

The system governing equations are solved by using C++ and EES to calculate the system performance and productivity parameters for different ranges of design and operating conditions as given in Table I.

TABLE I. STUDIED AND OPERATING PARAMETER VALUES

Parameter	Value
Turbine inlet temperature, t_{19}	170-195°C
Ambient air inlet temperature, t_1	25-45°C
Ambient air inlet humidity, w_1	12-20g$_v$/kga
Sea water inlet temperature, t_{13}	15-25°C
Evaporation pressure of ORC, P_{18}	200-400kPa
Condensation pressure of ORC, P_{17}	5-20kPa
ORC fluid mass flow rate, $\dot{m}_{ORC}$	0.5-1.3kg/s
Mass flow rate ratio, MR	0.1-0.6

IV. MODEL VALIDATION

To approve the developed thermodynamic models in the present work and to determine their degree of accuracy, model validation is applied and the results of the current work are compared with those reported in the literature. The validation of the current thermodynamic models with previously published data in [27, 29, 30] for HDH, ORC, and DCS subsystems is shown in Figure 3. It can be seen that there is good agreement between the current study's results and those previously reported in the literature.

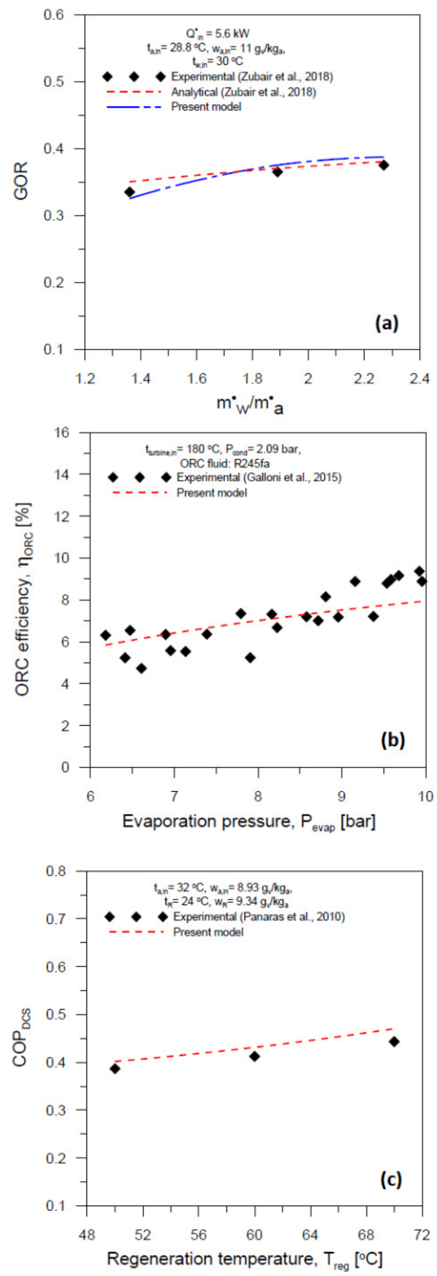

Fig. 3. Validation of the present model with the previously published data for (a) HDH, (b) ORC, (c) DCS.

V. RESULTS AND DISCUSSION

A comprehensive parametric study was conducted to study the effects of operating parameters on the performance of the proposed tri-generation system. For this purpose, the effects of turbine inlet temperature (t_{19}) of the ORC, ambient air inlet temperature and humidity ratio (t_1 and w_1), evaporation pressure (P_{18}) of the ORC, condensation pressure (P_{17}) of the ORC and mass flow rate ratio (MR) on the main productivity and performance parameters ($W^{\bullet}_{net}$, h_{ORC}, $m^{\bullet}_{fresh}$, GOR, $Q^{\bullet}_{cooling}$, COP_{DCS}, t_4, w_4, EUF_{PS}, and A_{PSC}) in addition to system assessment parameters (EUF_{imp}, $A_{SC,\text{sav}}$) are presented in Figures 4-10. The other parameters remain constant when a certain operating parameter is changed, in order to examine its effect. The performance parameters of the tri-generation system are investigated and evaluated with n-Octane as the working fluid in the ORC.

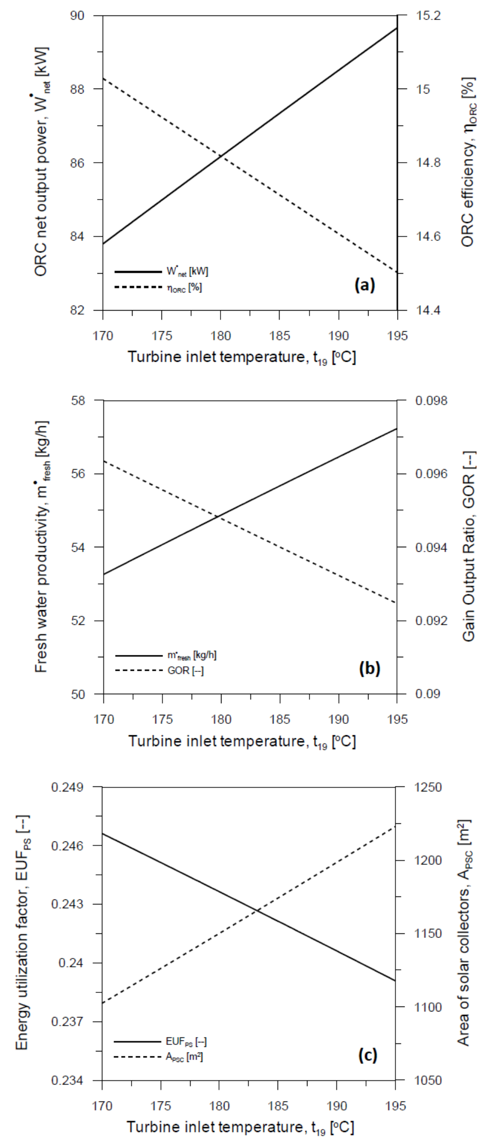

Fig. 4. Influence of t_{19} on the proposed system performance parameters.

A. *Effects of Turbine Inlet Temperature*

Figure 4 shows the effects of turbine inlet temperature (t_{19}) of the ORC on the main productivity and performance parameters of the proposed tri-generation system. t_{19} is increased from the fluid's saturated vapour temperature (170°C) to the superheated temperature (195°C). As shown in Figure 4, increasing t_{19} raises $W^{\bullet}_{net}$, $m^{\bullet}_{fresh}$, and A_{PSC}. The increase of the ORC turbine power, required input solar energy, and reject energy of the ORC condenser with increasing t_{19}, leading to the increase of ORC net output power, required area of solar collectors, humidification capacity of the air in the humidifier, and space cooling capacity. Also, the increase in heat input to ORC, HDH, and DCS with increasing turbine inlet temperature, leads to the reduction of h_{ORC}, *GOR*, and EUF_{PS}. It is found that the highest values of $W^{\bullet}_{net}$, h_{ORC}, $m^{\bullet}_{fresh}$, *GOR*, EUF_{PS}, and A_{PSC} are 89.66kW, 15.03%, 57.23kg/h, 0.09634, 0.2466, and 1223m^2 respectively, while their lowest are 83.8kW, 14.5%, 53.26kg/h, 0.09246, 0.2391, and 1102m^2. Furthermore, increasing t_{19} from 170°C to 195°C increased net output power, fresh water productivity, and space cooling capacity by 7%, 7.5%, and 10.3% respectively.

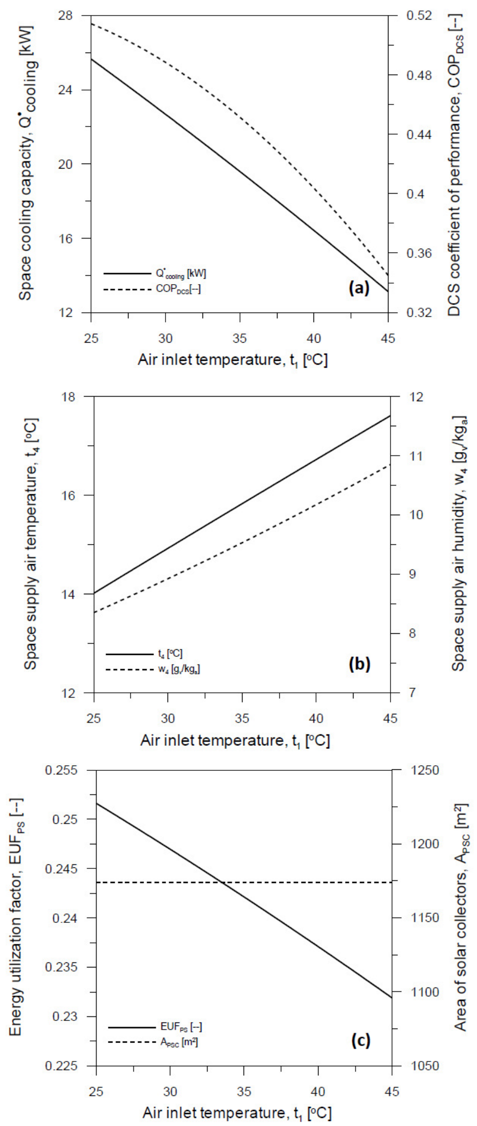

Fig. 5. Influence of t_1 on the proposed system performance parameters.

B. *Effect of Air Inlet Temperature*

The effect of the air inlet temperature on the main productivity and performance parameters of the proposed tri-generation system are given in Figure 5, which shows that as the air inlet temperature rises, the $Q^{\bullet}_{cooling}$, COP_{DCS}, and EUF_{PS} decrease while t_4 and w_4 increase, due to the increased required regeneration energy in DCS with increasing air inlet temperature, while the heat rejected in the condenser of ORC is fixed, leading to poor DCS performance. In addition, the highest obtained values of $Q^{\bullet}_{cooling}$, COP_{DCS}, t_4, w_4 and EUF_{PS} are 25.64kW, 0.5146, 17.61°C, 10.85g$_v$/kg$_a$ and 0.2516 respectively, while the lowest are 13.13kW, 0.3446, 14.02°C, 8.354g$_v$/kg$_a$ and 0.2319, where A_{PSC} is kept constant at 1174m^2. Furthermore, the fresh water productivity, $m^{\bullet}_{fresh}$, improved by 2.2% and the space cooling capacity, $Q^{\bullet}_{cooling}$, dropped by 48.9% with an increase of t_1 from 25°C to 45°C.

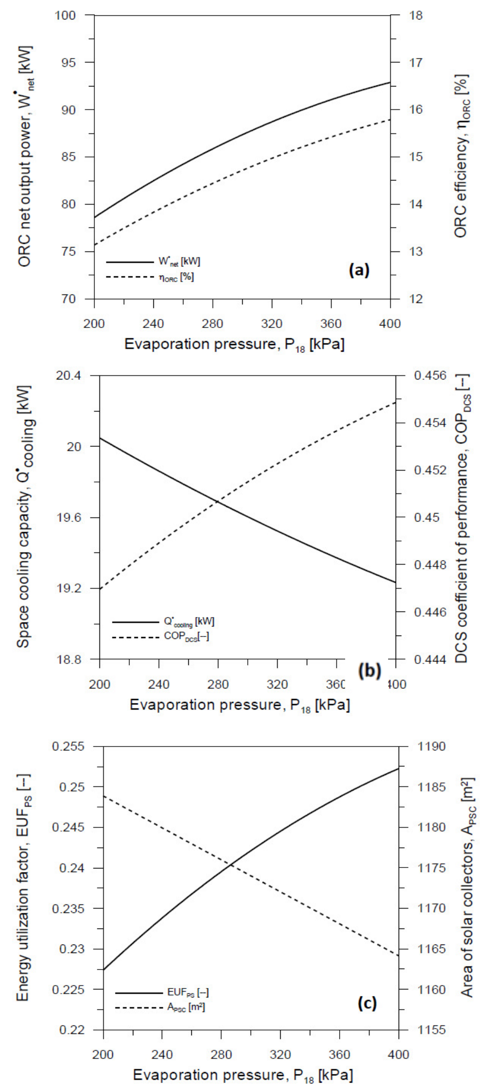

Fig. 6. Influence of P_{18} on the proposed system performance parameters.

C. *Effect of Evaporation Pressure*

The influence of the ORC evaporation pressure on the main productivity and performance parameters of the proposed tri-generation system is presented in Figure 6. The increase of $W^{\bullet}_{net}$, h_{ORC}, COP_{DCS}, and EUF_{PS} with the rise of the evaporation pressure can be seen. This occurs due to the decrease in heat input in the evaporator and heat reject in the condenser of ORC and the increased output power of the turbine. Figures 5(b)-(c) show the decrease of $Q^{\bullet}_{cooling}$ and A_{PSC} with the increase of the evaporation pressure. This can be attributed to the decrease of input heat to the ORC evaporator and the rejected heat from the condenser, which leads to a decrease in the humidification capacity of the air inside the humidifier and the fresh water yield in the dehumidifier. Hence, lower fresh water production rate can be obtained. Additionally, this reduces the regeneration energy of DCS and the required area of solar collectors. The highest obtained values of $W^{\bullet}_{net}$, h_{ORC}, $Q^{\bullet}_{cooling}$, COP_{DCS}, $EUFPS$, and A_{PSC} are 92.97kW, 15.8%, 20.05kW, 0.4469, 0.2524, and 1184m^2 respectively, while their lowest values are 87.34kW, 13.12%, 19.23kW, 0.4549, 0.2272, and 1164m^2. Furthermore, $W^{\bullet}_{net}$ improved by 6.4%, and $m^{\bullet}_{fresh}$ and $Q^{\bullet}_{cooling}$ dropped by 3.2% and 4.2% respectively when P_{18} increased from 200 to 400kPa.

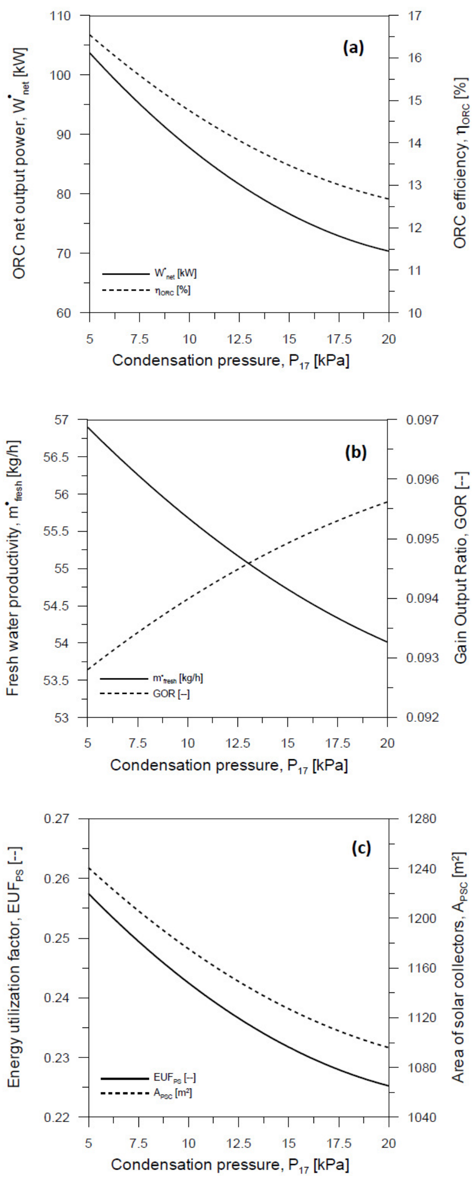

Fig. 7. Influences of P_{17} on the proposed system performance parameters.

D. Effects of ORC Condensation Pressure

Figure 7 shows the influence of ORC condensation pressure (P_{17}) on the proposed system performance and productivity parameters. $W^{\bullet}_{net}$, h_{ORC}, $m^{\bullet}_{fresh}$, EUF_{PS}, and A_{PSC} decrease as P_{17} increases. The reduction in net output power with increasing P_{17} is caused by the reduction in enthalpy difference across the turbine that leads to a reduction in ORC thermal efficiency. Decreasing the fresh water rate with rising condenser pressure is expected because of the reduced amount of heat recovered from the condenser to water and air streams before entering the humidifier, which lessens the amount of water evaporation and consequently reduces the amount of fresh water produced at the dehumidifier. The reduction in EUF_{PS} is attributed to the reducing of $W^{\bullet}_{net}$ and $m^{\bullet}_{fresh}$ with increasing P_{17}, which overcomes the reduction in the total input power of the system. The reduction in A_{PSC} with rising P_{17} is due to the reduction in the heat added to the evaporator at the same solar intensity input to the solar collectors. While Figure 7(b) displays increasing GOR with rising P_{17}, the increase in GOR is due to a decrease in both fresh water production rate and heating input power to the system that is needed to raise the temperatures of seawater and air to the humidifier inlet. The disadvantage of a decrease in fresh water production rate cannot compensate for the benefit of a decrease in system input power. It is observed that the highest $W^{\bullet}_{net}$, $m^{\bullet}_{fresh}$, and EUF_{PS} obtained at P_{17} = 5kPa are 104.5kW, 56.9 kg/h, and 0.2582 respectively, while the A_{PSC} reduction is 11.98% when the condenser pressure increases from 5 to 20kPa.

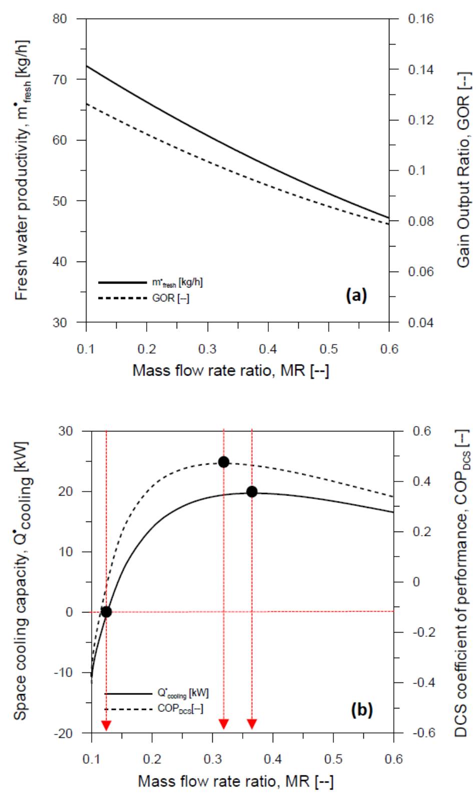

Fig. 8. Influence of MR on the proposed system performance parameters.

E. Effects of Mass Flow Rate Ratio

Figure 8 shows the influence of mass flow rate ratio (MR) on the proposed system performance and productivity parameters. Figure 8(a) shows the decrease of $m^{\bullet}_{fresh}$ and GOR with increasing MR. Increasing MR means lowering both the air and seawater mass flow rates equally (i.e. $m^{\bullet}_{a}= m^{\bullet}_{w}$) while keeping $m^{\bullet}_{ORC}$ constant and equal to 1kg/s, results in a lower rate of evaporation in the humidifier and a lower rate of condensation in the dehumidifier, and thus lower GOR. Figure 8(b) shows that $Q^{\bullet}_{cooling}$ and COP_{DCS} increase with increasing MR until they reach their highest values and then they decrease with increasing MR. Increasing MR has two opposing effects: i) it decreases the air mass flow rate and ii) it decreases the supply air enthalpy to the conditioned space, increasing the enthalpy difference across the conditioned space. As observed in Figure 8(b), for MR=0.38, the increase in enthalpy difference across the conditioned space overcomes the reduction in air mass flow rate, which results in higher $Q^{\bullet}_{cooling}$ and subsequently COP_{DCS}, and vice versa for MR>0.38. Furthermore, MR=0.125 leads to negative cooling capacity, which isn't recommended for cooling and dehumidifying applications through the conditioned space. It's noticed from Figure 8 that the maximum $m^{\bullet}_{fresh}$ and $Q^{\bullet}_{cooling}$ obtained are 72.13kg/h and 19.7kW and $m^{\bullet}_{fresh}$ improved by 52.7% when MR dropped from 0.6 to 0.1.

F. Effects of Ambient Air Humidity Ratio

Figure 9 depicts the effects of ambient air humidity ratio (w_1) variation with MR on the proposed system performance parameters. $Q^{\bullet}_{cooling}$, COP_{DCS}, and EUF_{PS} increase with increasing MR until they reach their highest values, and then they decrease with increasing MR for any w_1. Also, it is found that they drop with increasing w_1 for any MR. Increasing w_1 for the same MR increases the enthalpy of supply air, which reduces the air enthalpy difference through the conditioned space, which adversely effects the conditioned space cooling capacity as well as COP_{DCS} as seen in Figures 9(a)-(b). Moreover, the system operation conditions with MR less than 0.11, 0.15, 0.2, 0.25, at w_1 = 14, 16, 18, and 20g_v/kg_a respectively, are not recommended for cooling and dehumidifying applications due to the negative cooling capacity for the conditioned space. Furthermore, the highest values of $Q^{\bullet}_{cooling}$ that can be obtained are 26.46, 21.65, 17.93, 14.97, and 12.47kW at MR = 0.2667, 0.3222, 0.3778, 0.4889, 0.5444, and w_1 = 12, 14, 16, 18, and 20g_v/kg_a respectively. While increasing w_1 causes a decrease in EUF_{PS} because total system power output decreases when compared to the total system input power. Increasing w_1 causes a decrease in $Q^{\bullet}_{cooling}$ and an increase in $m^{\bullet}_{fresh}$ but $W^{\bullet}_{net}$ doesn't change, and the increase in $m^{\bullet}_{fresh}$ can't compensate for the reduction in $Q^{\bullet}_{cooling}$, which results in an adverse effect on EUF_{PS} as shown in Figure 9(c). At MR= 0.19, 0.24, 0.2667, 0.3222, 0.3778, and w_1= 12, 14, 16, 18, and 20gv/kga, the optimum EUF_{PS} values are 0.2643, 0.2526, 0.2435, 0.2356, and 0.2286. Additionally, w_1 has no effect on the A_{PSC} due to the independence of w_1 on the heating energy needed at the ORC evaporator.

G. System Assessment and Evaluation

To the best of our knowledge there are no tri-generation systems for power generation, A/C, and freshwater production systems available in the literature using ORC, DCS, and HDH combined integrated systems with the same operating conditions. Therefore, the performance of the proposed system is compared with the performance of a basic tri-generation system in which the needed heating sources for the three subsystems are taken separately from one source (i.e. solar collector system) that gathers the whole three subsystems into one basic tri-generation system, and the used system performance parameters are EUF_{BS} and A_{BSC} (see (34)-(35)). Therefore, the proposed system can be evaluated and assessed at different significant influencing operating parameters (t_{19}, P_{18}, and P_{17}) by using two important dimensionless performance and design parameters: Energy Utilization Factor improvement, EUF_{imp} (36), and solar collector area saving $A_{SC,sav}$ (37). As seen in Figures 10(a)-(b), EUF_{imp} and $A_{SC,sav}$ are enhanced with increasing t_{19} and P_{17}, due to the prevailing total energy output increment and solar collector area reduction of the proposed system than the basic system with increasing t_{19} and P_{17}, and the maximum values of EUF_{imp} that can be obtained are 68.4% and 69.9% at t_{19} = 195°C and P_{17} = 20kPa.

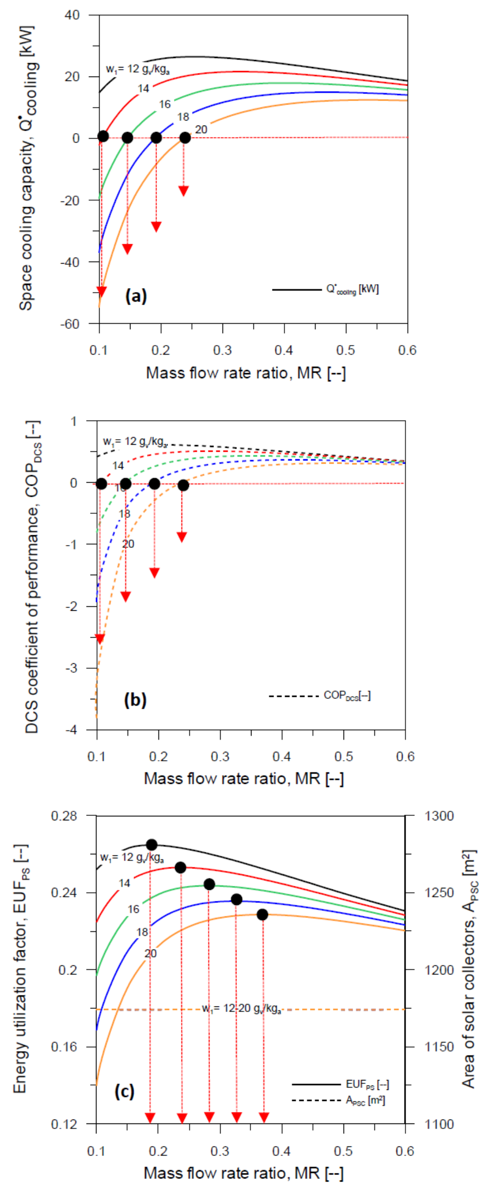

Fig. 9. Influence of w_1 on the proposed system performance parameters at MR values.

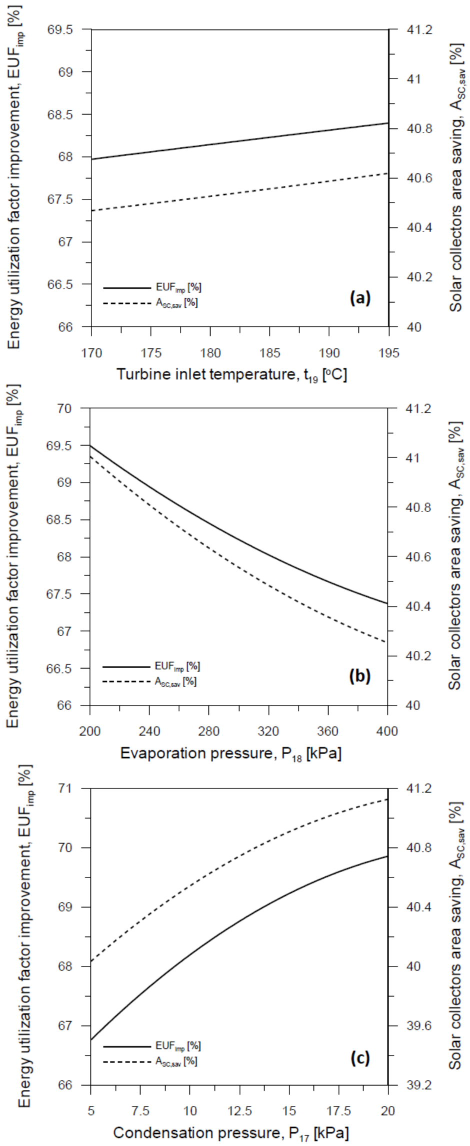

Fig. 10. Influences of studied system parameters on EUF_{imp} and $A_{SC,sav}$ of the proposed tri-generation system.

Similarly, the maximum values of $A_{SC,sav}$ that can be obtained are 40.62% and 41.14% at t_{19} = 195°C and P_{17} = 20kPa respectively. In addition, Figure 10(b) shows that increasing P_{18} has an adverse effect on EUF_{imp} and $A_{SC,sav}$ due to the advantage of EUF_{PS} increase and A_{PSC} reduction with rising P_{18} that can't compensate for the increasing of EUF_{BS} and decreasing of A_{BSC} that lead to decreasing EUF_{imp} and $A_{SC,sav}$ with rising P_{18}.

Table II illustrates the different values for EUF_{imp} and $A_{SC,sav}$ as system evaluation parameters for different operation and design parameters (t_1, t_{13}, $m^{\bullet}_{ORC}$, MR, w_1) that have no variation effects on EUF_{imp} and $A_{SC,sav}$ within their studied ranges. According to the Table, the maximum EUF_{imp} and $A_{SC,sav}$ obtained are 69.9% and 41.14% at t_{19} = 185°C, P_{18} = 300kPa, and P_{17} = 20kPa, and the minimum values obtained are 66.7% and 40.01% at t_{19} = 185°C, P_{18}= 300kPa, and P_{17}= 5kPa for all studied ranges of t_1, $m^{\bullet}_{ORC}$, MR, and w_1 .

TABLE II. PROPOSED SYSTEM ASSESSMENT AND EVALUATION FOR DIFFERENT PARAMETER VALUES

Parameter	t_{19} [°C]	P_{18} [kPa]	P_{17} [kPa]	EUF_{imp} [%]	$A_{SC,sav}$ [%]
t_1 (25-45 °C) t_{13} (15-25 °C) $m^{\bullet}_{ORC}$ (0.5-1.3 kg/s) MR (0.1-0.6) w_1 (12-20 g_v/kg_a)	170	300	10	67.97	40.47
	185	300	10	68.23	40.56
	195	300	10	68.4	40.62
	185	200	10	69.51	41.01
	185	400	10	67.36	40.25
	185	300	5	66.7	40.01
	185	300	20	69.9	41.14

H. Numerical Correlations Prediction

The numerical results are regressed to obtain new numerical correlations for the proposed tri-generation productivity and performance parameters ($W^{\bullet}_{net}$, $m^{\bullet}_{fresh}$, $Q^{\bullet}_{cooling}$, T_4, W_4, $A_{PSC,}$ and EUF_{PS}) in terms of all studied design and operating parameters. The obtained correlations with their errors are shown in Figure 11, and the presented correlations are valid in the ranges given in Table I, and the values of $t_{19,max}$, $t_{1,max}$, $t_{13,max}$, $m^{\bullet}_{ORC,max}$, $w_{1,max}$, are 195°C, 45°C, 25°C, 1.3kg/s, and 20 g_v/kg_a respectively.

Numerical correlations	Error
$W^{\bullet}_{net}\left[kW\right]=44.92\left(\frac{P_{18}}{P_{17}}\right)^{0.28}\left(\frac{t_{19}}{t_{19,max}}\right)^{0.49}\left(\frac{m^{\bullet}_{ORC}}{m^{\bullet}_{ORC,max}}\right)$	Predicts 100% of the numerical results within error ± 3%.
$A_{PSC}\left[m^2\right]=1248.15\left(\frac{P_{18}}{P_{17}}\right)^{0.071}\left(\frac{t_{19}}{t_{19,max}}\right)^{0.75}\left(\frac{m^{\bullet}_{ORC}}{m^{\bullet}_{ORC,max}}\right)$	Predicts 100% of the numerical results within error ± 3%.
$t_4\left[{}^{o}C\right]=16.4\,MR^{-0.21}\left(\frac{P_{18}}{P_{17}}\right)^{-0.005}\left(\frac{t_{19}}{t_{19,max}}\right)^{-0.16}\left(\frac{t_1}{t_{1,max}}\right)^{0.38}\left(\frac{t_{13}}{t_{13,max}}\right)^{-0.045}\left(\frac{w_1}{w_{1,max}}\right)^{0.44}$	Predicts 100% of the numerical results within error ± 2.7%.
$w_4\left[g_v/kg_a\right]=9.1\,MR^{-0.36}\left(\frac{P_{18}}{P_{17}}\right)^{-0.01}\left(\frac{t_{19}}{t_{19,max}}\right)^{-0.26}\left(\frac{t_1}{t_{1,max}}\right)^{0.46}\left(\frac{t_{13}}{t_{13,max}}\right)^{-0.08}\left(\frac{w_1}{w_{1,max}}\right)^{0.54}$	Predicts 100% of the numerical results within error ± 5%.
$EUF_{PS}\left[-\right]=0.143\,MR^{-0.04}\left(\frac{P_{18}}{P_{17}}\right)^{0.11}\left(\frac{t_{19}}{t_{19,max}}\right)^{-0.28}\left(\frac{t_1}{t_{1,max}}\right)^{-0.14}\left(\frac{t_{13}}{t_{13,max}}\right)^{-0.1}\left(\frac{w_1}{w_{1,max}}\right)^{-0.17}$	Predicts 99% of the numerical results within error ± 5%.
$m^{\bullet}_{fresh}\left[kg/h\right]=50.75\,MR^{-0.25}\left(\frac{P_{18}}{P_{17}}\right)^{0.02}\left(\frac{t_{19}}{t_{19,max}}\right)^{0.5}\left(\frac{t_1}{t_{1,max}}\right)^{0.034}\left(\frac{t_{13}}{t_{13,max}}\right)^{-0.45}\left(\frac{w_1}{w_{1,max}}\right)^{0.042}\left(\frac{m^{\bullet}_{ORC}}{m^{\bullet}_{ORC,max}}\right)$	Predicts 97% of the numerical results within error ± 5%.
$Q^{\bullet}_{cooling}\left[kW\right]=16.68\,MR^{0.22}\left(\frac{P_{18}}{P_{17}}\right)^{-0.013}\left(\frac{t_{19}}{t_{19,max}}\right)^{0.27}\left(\frac{t_1}{t_{1,max}}\right)^{-1.034}\left(\frac{t_{13}}{t_{13,max}}\right)^{0.17}\left(\frac{w_1}{w_{1,max}}\right)^{-1.35}\left(\frac{m^{\bullet}_{ORC}}{m^{\bullet}_{ORC,max}}\right)$	Predicts 90% of the numerical results within error ± 15%.

Fig. 11. Numerical correlation predictions and their errors.

VI. CONCLUSION AND RECOMMENDATIONS

In this article, an innovative combined ORC, DCS, and HDH tri-generation solar-driven plant for electrical power, cooling, and desalinated water production was presented. The proposed system recovers the ORC condenser heat to be used as a heating source and prime mover of the DCS and HDH sub systems. The proposed system's performance was evaluated and compared with the basic tri-generation system to find the optimum system operation conditions. The major concluding remarks of the current study are:

- The proposed tri-generation system can produce electrical power and fresh water and carry out the space cooling load while keeping comfortable conditions inside the space.
- The net output power increases with increasing turbine inlet temperature, ORC evaporation pressure, and ORC fluid flow rate, and it decreases with ORC condensation pressure and does not affect ambient air inlet temperature, or mass flow rate ratio.
- Fresh water productivity improved with rising turbine inlet temperature and ambient air inlet temperature, while it decreased with mass flow rate ratio, ORC condensation pressure, and ORC evaporation pressure.
- Space cooling load is enhanced at higher turbine inlet temperature, ORC fluid flow rate, and mass flow rate ratio and it decreases with increasing ambient air humidity ratio, ORC condensation pressure, and ORC evaporation pressure.
- The proposed system can provide maximum electrical power, fresh water, cooling capacity, and energy utilization factor of 104.5kW, 72.37kg/h, 25.48kW, and 0.2421 respectively at t_{19} = 185°C, t_1 = 35°C, w_1 = 15g$_v$/kg$_a$, t_{13} = 20°C, P_{18} = 300kPa, P_{17} = 10kPa, MR = 0.4, and $\dot{m}_{ORC}$ = 1kg/s.
- With increasing t_{19} from 170°C to 195°C, net output power, fresh water productivity, and space cooling capacity improved by 7%, 7.5%, and 10.3% respectively.
- $\dot{m}_{fresh}$ increased by 2.2% and space cooling capacity $\dot{Q}_{cooling}$ decreased by 48.9% when t_1 increased from 25 to 45°C.
- Increasing P_{18} from 200 to 400kPa, $\dot{m}_{fresh}$ and $\dot{Q}_{cooling}$ dropped by 3.2% and 4.20% respectively.
- MR should be 0.21 at $w_1 = 15g_v/kg_{da}$ for cooling applications because the supply air humidity ratio (w_4) should be equal to or less than the room humidity ratio (w_5 = 12g$_v$/kg$_a$). Moreover, the system operation conditions with MR less than 0.11, 0.15, 0.2, 0.25, at w_1 = 14, 16, 18, and 20g$_v$/kg$_a$ respectively, are not recommended for cooling and dehumidifying applications due to the negative cooling capacity for the conditioned space.
- The energy utilization factor increased as the ORC evaporation pressure and mass flow rate ratio increased (for MR = 0.2667 at w_1 = 15g$_v$/kg$_a$), and decreased as the ORC condensation pressure, ambient air inlet temperature and humidity, turbine inlet temperature, and mass flow rate ratio decreased.
- The highest energy utilization factor attained is 0.2643 at t_{19} = 185°C, t_1 = 35°C, t_{13} = 20°C, P_{17} = 10kPa, P_{18} = 300kPa, $\dot{m}_{ORC}$ = 1kg/s, MR = 0.19, and w_1 = 12g$_v$/kg$_a$.
- With increasing turbine inlet temperature and ORC condensation pressure, system evaluation performance parameters (EUF_{imp} and $A_{SC,sav}$) improved, but they dropped at higher ORC evaporation pressure. At t_{19} = 185°C, P_{18} = 300kPa, and P_{17} = 20kPa, the maximum EUF_{imp} and $A_{SC,sav}$ obtained are 69.9% and 41.14% respectively.
- Finally, general numerical correlations obtained from the numerical data can predict the system's productivity and system performance parameters with reasonable error.

Experimental and transient analyses using more heat recovery approaches are recommended as future work for the proposed system.

ACKNOWLEDGEMENT

This work was funded by the University of Jeddah, Jeddah, Saudi Arabia, under grant No. UJ-20-015-DR. The authors thank the University for the technical and financial support.

NOMENCLATURE

A	Area, m^2
Cp	Specific heat, kJ/kg K
F_1, F_2	Combined potential, -
h_{fg}	Water latent heat of evaporation, kJ/kg
h	Specific enthalpy, kJ/kg
I_T	Total solar intensity, W/m^2
$\dot{m}$	Mass flow rate, kg/s
$\dot{Q}$	Heat transfer rate, kW
t	Temperature, °C
W	Humidity ratio, g$_v$/kg$_a$
$\dot{W}$	Power, kW
β	Tilt angle, °
η	Efficiency
η_{F1}, η_{F2}	Efficiency of the desiccant wheel
ε	Effectiveness
τ	Time, hours
	Subscript
a	Air/dry air/actual
atm	Atmosphere
avg	Average
BS	Basic system
BSC	Basic Solar Collectors
$cond$	Condenser
$Evap$	Evaporator
g	Generator
hum	Humidifier
HE	Heat exchanger
i= 1,2,3	Index referring to various positions of the desiccant system
imp	Improvement
in	Input
ma	Moist air
v	Water vapour
reg	Regeneration
R,a	Return air
P,a	Process air
P	Pump
PS	Proposed system
PSC	Proposed solar collectors
SC	Solar collectors
Sav	Saving

t	Turbine
w	Seawater
1, 2, 3, ……	State points

Abbreviations

DCS	Desiccant Cooling System
DEC	Direct Evaporative Cooler
EUF	Energy Utilization Factor
COP	Coefficient Of Performance
GOR	Gain Output Ratio
HDH	Humidification Dehumidification
KSA	Kingdom of Saudi Arabia
ORC	Organic Rankine Cycle
MR	Mass flow rate ratio

REFERENCES

[1] Y. Wang and N. Lior, "Performance analysis of combined humidified gas turbine power generation and multi-effect thermal vapor compression desalination systems — Part 1: The desalination unit and its combination with a steam-injected gas turbine power system," *Desalination*, vol. 196, no. 1, pp. 84–104, Sep. 2006, https://doi.org/10.1016/j.desal.2006.01.010.

[2] Y. Wang and N. Lior, "Performance analysis of combined humidified gas turbine power generation and multi-effect thermal vapor compression desalination systems," *Desalination*, vol. 1–3, no. 207, pp. 243–256, 2007, https://doi.org/10.1016/j.desal.2006.06.013.

[3] R. Chacartegui, D. Sanchez, N. di Gregorio, F. J. Jimenez-Espadafor, A. Munoz, and T. Sanchez, "Feasibility analysis of a MED desalination plant in a combined cycle based cogeneration facility," *Applied Thermal Engineering*, vol. 29, no. 2, pp. 412–417, Feb. 2009, https://doi.org/10.1016/j.applthermaleng.2008.03.013.

[4] E. A. Al-Ammar, N. H. Malik, and M. Usman, "Application of using Hybrid Renewable Energy in Saudi Arabia," *Engineering, Technology & Applied Science Research*, vol. 1, no. 4, pp. 84–89, Aug. 2011, https://doi.org/10.48084/etasr.33.

[5] J. B. V. Subrahmanyam, P. Alluvada, Bandana, K. Bhanupriya, and C. Shashidhar, "Renewable Energy Systems: Development and Perspectives of a Hybrid Solar-Wind System," *Engineering, Technology & Applied Science Research*, vol. 2, no. 1, pp. 177–181, Feb. 2012, https://doi.org/10.48084/etasr.104.

[6] A. Belkadi, D. Mezghani, and A. Mami, "Energy Design and Optimization of a Greenhouse: A Heating, Cooling and Lighting Study," *Engineering, Technology & Applied Science Research*, vol. 9, no. 3, pp. 4235–4242, Jun. 2019, https://doi.org/10.48084/etasr.2787.

[7] M. Ray, P. Samal, and C. K. Panigrahi, "Implementation of a Hybrid Technique for the Predictive Control of the Residential Heating Ventilation and Air Conditioning Systems," *Engineering, Technology & Applied Science Research*, vol. 12, no. 3, pp. 8772–8776, Jun. 2022, https://doi.org/10.48084/etasr.5027.

[8] P. Palenzuela, G. Zaragoza, and D.-C. Alarcon-Padilla, "Characterisation of the coupling of multi-effect distillation plants to concentrating solar power plants," *Energy*, vol. 82, pp. 986–995, Mar. 2015, https://doi.org/10.1016/j.energy.2015.01.109.

[9] A. Fouda, S. A. Nada, and H. F. Elattar, "An integrated A/C and HDH water desalination system assisted by solar energy: Transient analysis and economical study," *Applied Thermal Engineering*, vol. 108, pp. 1320–1335, Sep. 2016, https://doi.org/10.1016/j.applthermaleng.2016.08.026.

[10] H. F. Elattar, A. Fouda, and S. A. Nada, "Performance investigation of a novel solar hybrid air conditioning and humidification–dehumidification water desalination system," *Desalination*, vol. 382, pp. 28–42, Mar. 2016, https://doi.org/10.1016/j.desal.2015.12.023.

[11] S. A. Nada, H. F. Elattar, and A. Fouda, "Energy-efficient hybrid A/C and freshwater production system proposed for high latent load spaces," *International Journal of Energy Research*, vol. 43, no. 13, pp. 6812–6826, 2019, https://doi.org/10.1002/er.4677.

[12] H. F. Elattar, S. A. Nada, A. Al-Zahrani, and A. Fouda, "Humidification-dehumidification water desalination system integrated with multiple evaporators/condensers heat pump unit," *International Journal of Energy Research*, vol. 44, no. 8, pp. 6396–6416, 2020, https://doi.org/10.1002/er.5368.

[13] S. A. Nada, A. Fouda, M. A. Mahmoud, and H. F. Elattar, "Experimental investigation of air-conditioning and HDH desalination hybrid system using new packing pad humidifier and strips-finned helical coil," *Applied Thermal Engineering*, vol. 185, Feb. 2021, Art. no. 116433, https://doi.org/10.1016/j.applthermaleng.2020.116433.

[14] M. Jradi and S. Riffat, "Tri-generation systems: Energy policies, prime movers, cooling technologies, configurations and operation strategies," *Renewable and Sustainable Energy Reviews*, vol. 32, pp. 396–415, Apr. 2014, https://doi.org/10.1016/j.rser.2014.01.039.

[15] S. Sibilio, A. Rosato, G. Ciampi, M. Scorpio, and A. Akisawa, "Building-integrated trigeneration system: Energy, environmental and economic dynamic performance assessment for Italian residential applications," *Renewable and Sustainable Energy Reviews*, vol. 68, pp. 920–933, Feb. 2017, https://doi.org/10.1016/j.rser.2016.02.011.

[16] G. Leonzio, "An innovative trigeneration system using biogas as renewable energy," *Chinese Journal of Chemical Engineering*, vol. 26, no. 5, pp. 1179–1191, May 2018, https://doi.org/10.1016/j.cjche.2017.11.006.

[17] M. S. Azhar, G. Rizvi, and I. Dincer, "Integration of renewable energy based multigeneration system with desalination," *Desalination*, vol. 404, pp. 72–78, Feb. 2017, https://doi.org/10.1016/j.desal.2016.09.034.

[18] B. Ghorbani, M. Mehrpooya, and M. Sadeghzadeh, "Developing a tri-generation system of power, heating, and freshwater (for an industrial town) by using solar flat plate collectors, multi-stage desalination unit, and Kalina power generation cycle," *Energy Conversion and Management*, vol. 165, pp. 113–126, Jun. 2018, https://doi.org/10.1016/j.enconman.2018.03.040.

[19] AymanO. Abdelhay, HassanE. S. Fath, and S. A. Nada, "Solar driven polygeneration system for power, desalination and cooling," *Energy*, vol. 198, May 2020, Art. no. 117341, https://doi.org/10.1016/j.energy.2020.117341.

[20] T. Gholizadeh, M. Vajdi, and H. Rostamzadeh, "A new trigeneration system for power, cooling, and freshwater production driven by a flash-binary geothermal heat source," *Renewable Energy*, vol. 148, pp. 31–43, Apr. 2020, https://doi.org/10.1016/j.renene.2019.11.154.

[21] I. Dincer and M. Demir, "4.8 Steam and Organic Rankine Cycles," in *Comprehensive Energy Systems*, Amsterdam, Netherlands: Elsevier, 2018, pp. 264–311.

[22] I. K. Karathanassis, E. Papanicolaou, V. Belessiotis, and G. C. Bergeles, "Design and experimental evaluation of a parabolic-trough concentrating photovoltaic/thermal (CPVT) system with high-efficiency cooling," *Renewable Energy*, vol. 101, pp. 467–483, Feb. 2017, https://doi.org/10.1016/j.renene.2016.09.013.

[23] M. A. Sharaf Eldean and A. M. Soliman, "Study of Using Solar Thermal Power for the Margarine Melting Heat Process," *Journal of Solar Energy Engineering*, vol. 137, no. 2, Sep. 2014, Art. no. 021004, https://doi.org/10.1115/1.4028367.

[24] M. Yari, L. Ariyanfar, and E. A. Aghdam, "Analysis and performance assessment of a novel ORC based multi-generation system for power, distilled water and heat," *Renewable Energy*, vol. 119, pp. 262–281, Apr. 2018, https://doi.org/10.1016/j.renene.2017.12.021.

[25] A. Fouda, S. A. Nada, H. F. Elattar, S. Rubaiee, and A. Al-Zahrani, "Performance analysis of proposed solar HDH water desalination systems for hot and humid climate cities," *Applied Thermal Engineering*, vol. 144, pp. 81–95, Nov. 2018, https://doi.org/10.1016/j.applthermaleng.2018.08.037.

[26] L. M. Ayompe and A. Duffy, "Thermal performance analysis of a solar water heating system with heat pipe evacuated tube collector using data from a field trial," *Solar Energy*, vol. 90, pp. 17–28, Apr. 2013, https://doi.org/10.1016/j.solener.2013.01.001.

[27] G. Panaras, E. Mathioulakis, V. Belessiotis, and N. Kyriakis, "Theoretical and experimental investigation of the performance of a desiccant air-conditioning system," *Renewable Energy*, vol. 35, no. 7, pp. 1368–1375, Jul. 2010, https://doi.org/10.1016/j.renene.2009.11.011.

[28] N. Wang *et al.*, "Performance assessment of PCM-based solar energy assisted desiccant air conditioning system combined with a humidification-dehumidification desalination unit," *Desalination*, vol. 496, Dec. 2020, Art. no. 114705, https://doi.org/10.1016/j.desal.2020.114705.

[29] S. M. Zubair, M. A. Antar, S. M. Elmutasim, and D. U. Lawal, "Performance evaluation of humidification-dehumidification (HDH) desalination systems with and without heat recovery options: An experimental and theoretical investigation," *Desalination*, vol. 436, pp. 161–175, Jun. 2018, https://doi.org/10.1016/j.desal.2018.02.018.

[30] E. Galloni, G. Fontana, and S. Staccone, "Design and experimental analysis of a mini ORC (organic Rankine cycle) power plant based on R245fa working fluid," *Energy*, vol. 90, pp. 768–775, Oct. 2015, https://doi.org/10.1016/j.energy.2015.07.104.